Description of inelastic scattering between heavy ions in the Glauber model

S. M. Lenzi
Dipartimento di Fisica, Università degli Studi di Padova, Padova, Italy
Istituto Nazionale di Fisica Nucleare, Padova, Italy
and Consejo Nacional de Investigaciones Científicas y Técnicas, Buenos Aires, Argentina

A. Vitturi
Dipartimento di Fisica, Università degli Studi di Trento, Trento, Italy
and Istituto Nazionale di Fisica Nucleare, Padova, Italy

F. Zardi
Dipartimento di Fisica, Università degli Studi di Padova, Padova, Italy
and Istituto Nazionale di Fisica Nucleare, Padova, Italy
(Received 22 July 1988)

The optical limit of the Glauber model is used for the description of inelastic processes in heavy-ion reactions at intermediate energies. Different prescriptions are investigated to obtain the inelastic scattering amplitude from the corresponding microscopic nucleon-nucleon amplitude. Besides the standard one in which the target excitation is ascribed to a projectile-nucleon collision and contributions from multiple-scattering processes are preliminarily summed to produce the elastic projectile-nucleon amplitude, we suggest the alternative approach in which a single nucleon-nucleon collision causes the inelastic transition. In all cases the formalism is modified to take into account the deflection of the classical orbits due to the strong repulsive Coulomb field. Parameter-free predictions for the inelastic excitation, based on experimental nucleon-nucleon total cross sections and standard densities, show a remarkable agreement with both experiment and distorted-wave Born approximation calculations.

I. INTRODUCTION

Experimental data for both elastic and inelastic collisions between heavy ions at intermediate energies (i.e., $E/A \approx 30-100$ MeV) have become available in the last few years.[1-3] They have been successfully described within the standard approaches based on the optical model and distorted-wave Born approximation (DWBA).[3] In a recent paper[4] the elastic scattering with heavy projectiles ($A > 4$) has been described within the Glauber model, with proper modifications to take into account the deflection of the classical orbits due to the strong repulsive Coulomb field. In this paper we discuss the use of the Glauber model in the description of inelastic channels, along a formalism previously used for light-projectile induced reactions.[5,6] Our aim is to show that, as in the case of elastic scattering,[7] all the dynamics of the inelastic process between heavy ions are, also at these intermediate energies, essentially governed by the nucleon-nucleon collisions, the other necessary information being given by the "static" nuclear densities and transition densities.

A crucial and open point in the description of inelastic processes within a nucleus-nucleus Glauber model is the choice of the microscopic reaction mechanism responsible for the transition. In the fully microscopic approach the contributions of multiple nucleon-nucleon collisions are summed to all orders as in the elastic case, but only one of the nucleon-nucleon collisions is assumed to cause the transition to the inelastic channel (for example, in the target), all the others being of elastic character. Within this approach, nucleons in the projectile and in the target are treated on the same footing, and the formalism is suited to be directly extended to mutual excitation processes, or to processes which can be formally described as a mutual excitation, as for example charge-exchange reactions. An alternative approach makes use of two successive applications of the nucleon-nucleus scattering formalism. The contributions of multiple nucleon-nucleon collisions are first summed to all possible orders to give the elastic amplitude for the collision of the projectile with a nucleon of the target, to be then used for the nucleus-nucleus inelastic scattering which is assumed to be induced by a single projectile-nucleon collision. The two approaches are derived and discussed in Sec. II.

Applications of the formalism are given in Sec. III. The predictions of the model for the excitation of the first 2^+ state in the $^{12}C + {}^{12}C$ reaction at 360 and 1016 MeV are compared with both experimental data and DWBA calculation. As an example of reactions involving heavily charged systems, the excitation of the target 2^+ state is considered in the $^{40}Ar + {}^{208}Pb$ reaction.

II. THE FORMALISM

A. Elastic scattering

A fruitful way of looking at the Glauber model for the elastic scattering of composite systems[8] is to derive it as an approximation to the multiple-scattering theory

developed by Golberger and Watson.[9] It is in fact possible to show[10] that the latter leads to the former in the high-energy limit under the assumptions of the eikonal and closure approximations and neglecting rescattering terms and off-shell effects. Under these hypotheses we can, in fact, obtain the standard Glauber expression for the elastic scattering amplitude between a projectile (P) and a target (T),

$$f_{00}(\bar{\Delta})=\frac{ik}{2\pi}\int d^2b\, e^{i\bar{\Delta}\cdot\bar{b}}\Gamma_{00}(\bar{b}) , \tag{1}$$

where

$$\Gamma_{00}(\bar{b})=\langle \Phi_0^T\Phi_0^P \mid \Gamma \mid \Phi_0^T\Phi_0^P\rangle \tag{2}$$

and

$$\Gamma=1-\prod_{i=1}^{A_T}\prod_{j=1}^{A_P}[1-\gamma(\bar{b}-\bar{s}_i-\bar{s}_j)] \tag{3}$$

in terms of the impact parameter $\bar{b}$ and the projections $\bar{s}$ of the nucleon intrinsic coordinates on the impact parameter plane. The elementary profile $\gamma(\bar{b})$ is connected to the nucleon-nucleon scattering amplitude in the form

$$\gamma(\bar{b})=\frac{1}{2\pi ik_{NN}}\int d^2q\, e^{-i\bar{q}\cdot\bar{b}}f_{NN}(\bar{q}) , \tag{4}$$

where k_{NN} is the nucleon-nucleon c.m. momentum.

Within this scheme, the optical limit of the model can be obtained by replacing in each term in Eq. (3) the closure approximation by the assumption of retaining in each intermediate completeness only the term corresponding to the ground state of both target and projectile.[11] This amounts to approximately the nth order scattering term

$$\Gamma_{00}^{(n)}=\langle \Phi_0^T\Phi_0^P \mid \gamma\gamma\cdots\gamma \mid \Phi_0^T\Phi_0^P\rangle ,$$

where n elementary profiles γ appear, by the factorized expression

$$\Gamma_{00}^{(n)}\approx\langle \Phi_0^T\Phi_0^P \mid \gamma \mid \Phi_0^T\Phi_0^P\rangle\langle \Phi_0^T\Phi_0^P \mid \gamma \mid \Phi_0^T\Phi_0^P\rangle\cdots\langle \Phi_0^T\Phi_0^P \mid \gamma \mid \Phi_0^T\Phi_0^P\rangle=[\lambda(b)]^n . \tag{5}$$

Within the independent particle model, the basic quantity $\lambda(b)$ can be expressed in terms of the nuclear densities in the form

$$\begin{aligned}\lambda(b)&=\int \rho_0^P(\bar{r}_P)\rho_0^T(\bar{r}_T)\gamma(\bar{b}-\bar{s}_P-\bar{s}_T)\,d\bar{r}_P d\bar{r}_T\\&=\frac{1}{2\pi ik_{NN}}\int \hat{\rho}_0^P(q)\hat{\rho}_0^T(q)f_{NN}(q)e^{-i\bar{q}\cdot\bar{b}}d\bar{q} ,\end{aligned} \tag{6}$$

having assumed a single particle density normalized to one and having defined as $\hat{\rho}_0^P(q)$ and $\hat{\rho}_0^T(q)$ the Fourier transform of the nuclear densities. This "frozen-nucleus" approximation leads to the well known optical-limit expression for the elastic scattering amplitude[8]

$$\begin{aligned}f_{00}(\bar{\Delta})&=\frac{ik}{2\pi}\int d^2b\, e^{i\bar{\Delta}\cdot\bar{b}}\{1-[1-\lambda(b)]^{A_T A_P}\}\\&\approx\frac{ik}{2\pi}\int d^2b\, e^{i\bar{\Delta}\cdot\bar{b}}[1-e^{iA_T A_P\lambda(b)}] .\end{aligned} \tag{7}$$

B. Inelastic scattering

A similar approach can be applied to the description of inelastic scattering processes. For simplicity we will consider the case of target excitation, but the formalism can easily be generalized to the case of projectile excitation, or mutual excitation. The amplitude associated with the excitation of the state $\mid LM\rangle$ gets in the Glauber model the expression

$$f_{LM,0}(\bar{\Delta})=\frac{ik}{2\pi}\int d^2b\, e^{i\bar{\Delta}\cdot\bar{b}}\langle \Phi_{LM}^T\Phi_0^P \mid \Gamma \mid \Phi_0^T\Phi_0^P\rangle , \tag{8}$$

where Φ_{LM}^T is the nuclear wave function associated with the state $\mid LM\rangle$. The optical limit can now be obtained by truncating each intermediate completeness to the sum of only two terms,

$$\mid \Phi_0^T\Phi_0^P\rangle\langle \Phi_0^T\Phi_0^P\mid + \mid \Phi_{LM}^T\Phi_0^P\rangle\langle \Phi_{LM}^T\Phi_0^P\mid . \tag{9}$$

We will assume now all the diagonal terms associated with both the ground and excited state are identical

$$\lambda(b)=\langle \Phi_0^T\Phi_0^P \mid \gamma \mid \Phi_0^T\Phi_0^P\rangle\approx\langle \Phi_{LM}^T\Phi_0^P \mid \gamma \mid \Phi_{LM}^T\Phi_0^P\rangle \tag{10}$$

and denote $\mu_{LM}(b)$ the nondiagonal terms

$$\mu_{LM}(b)=\langle \Phi_{LM}^T\Phi_0^P \mid \gamma \mid \Phi_0^T\Phi_0^P\rangle . \tag{11}$$

Within the assumption of weak coupling to the excited state, we will neglect now all the multiple scattering sequences where more than one nondiagonal term appears connecting the ground and the excited state in the target. This is, in spirit, equivalent to the first-order Born approximation in the standard scattering theory. In this way we get the final expression for the inelastic scattering amplitude

$$f_{LM,0}(\bar{\Delta})=\frac{ik}{2\pi}A_T A_P\int d^2b\, e^{i\bar{\Delta}\cdot\bar{b}}\mu_{LM}(b)[1-\lambda(b)]^{A_T A_P-1} . \tag{12}$$

Expliciting the right-hand side of Eq. (11) in the momentum space, and defining

$$\hat{\rho}_L^T(q)=4\pi\int dr\,[r^2 j_L(qr)\rho_L^T(r)] \tag{13}$$

in terms of the target transition density $\rho^T_{LM}(\bar{r})=\rho^T_L(r)Y_{LM}(\hat{r})$, we obtain

$$\mu_{LM}(b)=\frac{1}{ik}B_{LM}\int_0^\infty dq\, q\hat{\rho}^P_0(q)f_{NN}(q)\hat{\rho}^T_L(q)J_M(qb)\ , \tag{14}$$

where

$$B_{LM}=(-1)^M\left[\frac{2L+1}{4\pi}\right]^{1/2}\frac{[(L-M)!(L+M)!]^{1/2}}{(L-M)!!(L+M)!!}\left[\frac{1+(-1)^{L+M}}{2}\right]\ . \tag{15}$$

Note that the coefficients B_{LM} vanish for $L+M$ odd. This leads to the final expression for the inelastic cross section

$$\begin{aligned}(d\sigma/d\omega)_L&=\sum_{M=-L}^{L}|\,kA_TA_P\int_0^\infty db\, bJ_M(\Delta b)\mu_{LM}(b)[1-\lambda(b)]^{A_TA_P-1}\,|^2\\&\approx\sum_{M=-L}^{L}|\,kA_TA_P\int_0^\infty db\, bJ_M(\Delta b)\mu_{LM}(b)e^{i\lambda(b)A_TA_P}\,|^2\ .\end{aligned} \tag{16}$$

We remark that this approach corresponds to the assumption that a single nucleon-nucleon collision is responsible for the transition to the excited state, all the other collisions being of elastic character and therefore only contributing to generate the appropriate transmission coefficients. The approach displays the maximum symmetry between target and projectile, and is therefore the more suited to be extended to the case of mutual excitation, or to processes that can be formally described as mutual excitations, as for example charge-exchange reactions.

C. Semimicroscopic approach

An alternative and widely used approach to the description of inelastic scattering within the Glauber model is based on the frozen-projectile approximation.[5] This amounts to introduce an elementary nucleon-projectile profile and to assume that the excitation of the target is produced by a single collision of a target nucleon with the whole projectile. In this case the formalism derived for the nucleon-nucleus inelastic collisions[12] can be directly extended to describe the nucleus-nucleus scattering in the form

$$f_{LM,0}(\bar{q})=\frac{ik}{2\pi}A_T\int d^2b\, e^{i\bar{q}\cdot\bar{b}}g_{LM}(b)[1-\chi(b)]^{A_T-1}\ , \tag{17}$$

where

$$g_{LM}(b)=\frac{1}{ik_{NP}}B_{LM}\int qdq\, f_{NP}(q)\hat{\rho}^T_L(q)J_M(qb) \tag{18}$$

and

$$\chi(b)=\frac{1}{ik_{NP}}\int qdq\, f_{NP}(q)\hat{\rho}^T_0(q)J_0(qb)\ . \tag{19}$$

Both inelastic and elastic elements (18) and (19) are expressed in terms of the amplitude $f_{NP}(q)$ associated to the nucleon-projectile elastic scattering. The inelastic cross section is then expressed in the form

$$\begin{aligned}(d\sigma/d\omega)_L&=\sum_{M=-L}^{L}|\,kA_T\int_0^\infty db\, bJ_M(qb)g_{LM}(b)[1-\chi(b)]^{A_T-1}\,|^2\\&\approx\sum_{M=-L}^{L}|\,kA_T\int_0^\infty db\, bJ_M(qb)g_{LM}(b)e^{iA_T\chi(b)}\,|^2\ .\end{aligned} \tag{20}$$

Along the Glauber model, the nucleon-projectile amplitude f_{NP} can in turn be expressed in terms of the nucleon-nucleon scattering amplitude and the projectile density in the form

$$f_{NP}(q)=\frac{ik_{NP}}{2\pi}\int d^2b\, e^{i\bar{q}\cdot\bar{b}}\sum_{n=1}^{A_P}(-1)^{n+1}\Gamma_0^{(n)}\ , \tag{21}$$

where $\Gamma_0^{(n)}$ has the same structure as in Eq. (5), when one of the colliding nuclei is a nucleon.

The predictions for the inelastic cross section obtained from the two approaches summarized in formulas (16) and (20) are compared in a few examples in Sec. III. We note that keeping only first-order collisions in Eq. (21), i.e., assuming

$$f_{NP}(q)\approx\frac{k_{NP}}{k_{NN}}A_P\hat{\rho}^P_0(q)f_{NN}(q)\ , \tag{22}$$

and replacing it in Eqs. (18) and (19), it is immediate to regain from Eq. (20) the expression previously obtained in the fully microscopic approach. It is important to note however that this does not mean that the microscopic approach must be viewed as a first-order approximation to

the semimicroscopic approach, as it could appear from the above derivation. In fact, the two methods are deduced from different assumptions about the mechanism of the reaction and there is no *a priori* physical argument to state which of them is more suitable to describe the inelastic excitation process.

D. Modification due to the deflection of the trajectory by the Coulomb field

As apparent in the formalism, a basic assumption of the Glauber model is the description of the relative motion in terms of a straight line trajectory. Density and transition density overlaps (6) and (11) are in fact evaluated along straight lines associated with each impact parameter b. In the case of Gaussian shape for densities and elementary profiles, this leads to the additional bonus of analytical expressions. This straight-line assumption faces obvious limitations in the case of heavily charged systems at relatively low bombarding energies, a situation in which the distortion effects of the Coulomb field can by no means be neglected. As suggested in a previous paper on heavy-ion elastic scattering,[4] a simple although effective way of incorporating the focussing effect of the Coulomb field, without altering the simplicity of the straight-line model, is to evaluate all overlaps associated with a given impact parameter b using an effective impact parameter b'. This parameter b' corresponds to the distance of closest approach along pure Coulomb trajectory, and is related to b through

$$kb'=\eta+[\eta^2+k^2b^2]^{1/2} , \tag{23}$$

η being the Sommerfeld parameter. Therefore formulas (16) and (20) have to be rewritten in the form

$$(d\sigma/d\Omega)_L=\sum_{M=-L}^{L}\left|kA_TA_P\int_0^\infty db\, bJ_M(\Delta b)\mu_{LM}[b'(b)]e^{i\lambda[b'(b)]A_TA_P}\right|^2 , \tag{24}$$

$$(d\sigma/d\Omega)_L=\sum_{M=-L}^{L}\left|kA_T\int_0^\infty db\, bJ_M(qb)g_{LM}[b'(b)]e^{iA_T\chi[b'(b)]}\right|^2 , \tag{25}$$

where the function $b'(b)$ is obtained from (23).

In the case of heavy-ion reactions, which are mainly governed by the grazing collisions, this recipe leads to the correct grazing angular momentum, otherwise overestimated in the pure straight-line approach. The correct grazing angular momentum is in turn the necessary ingredient to obtain angular distributions which display the correct period of oscillation for diffractive-type reactions or the correct grazing angle for bell-shaped reactions. Examples of the effect of this correction on the inelastic scattering cross sections in both cases are given in Figs. 5 and 6.

III. APPLICATIONS

This section is devoted to the application of the formalism displayed in the previous section to a number of heavy-ion inelastic scattering collisions. In all the cases considered, the elastic scattering process has already been successfully described[4,13] within the Glauber model, and this is a further element for not treating as adjustable parameters the quantities defining the nucleon-nucleon interaction and the nuclear densities. Also in this case, therefore, we will assume an isotropic nucleon-nucleon scattering amplitude

$$f_{NN}(q)=\frac{\alpha_{NN}+i}{4\pi}k_{NN}\sigma_{NN} , \tag{26}$$

where σ_{NN} and α_{NN} are the total nucleon-nucleon cross section and the ratio of real to imaginary part of the forward nucleon-nucleon scattering amplitude. Both have to be evaluated at the corresponding energy of the microscopic collision, and have been taken from the nucleon-nucleon experimental data. Similarly, we have assumed a Gaussian form for the nuclear densities

$$\rho_0^i(r)=\rho_0^i(0)e^{-r^2/a_i^2}\quad (i=P,T) , \tag{27}$$

also for heavy systems like ^{40}Ar and ^{208}Pb. In these cases the Gaussian functions have been adjusted[14] to reproduce the corresponding Fermi densities on the nuclear surface, in the assumption that only this region will be important for grazing collisions. With these choices the elastic phase shift $\lambda(b)$ in (16) gets the simple analytic expression

$$\lambda(b)=\tfrac{1}{2}\sigma_{NN}(\alpha_{NN}+i)\Omega(b) , \tag{28}$$

where the density overlap $\Omega(b)$ is given by

$$\Omega(b)=\rho_0^P(0)\rho_0^T(0)\pi^2\frac{a_P^3a_T^3}{a_P^2+a_T^2}e^{-b^2/(a_P^2+a_T^2)} . \tag{29}$$

Simplifications also occur for the nondiagonal matrix elements. In the case of collective states described within the Tassie model, the transition density $\rho_L^T(r)$ and its transform $\hat{\rho}_L^T(q)$ assume the form

$$\rho_L^T(r)=\frac{\beta_L}{\sqrt{2L+1}}r^{L-1}\frac{d\rho_0^T(r)}{dr} \tag{30}$$

and

$$\hat{\rho}_L^T(q)=-2a_T\frac{\rho_0^T(0)\beta_L}{\sqrt{2L+1}}\pi^{3/2}\left[\frac{a_T^2}{2}\right]^L q^L e^{-(q^2a_T^2)/4} . \tag{31}$$

TABLE I. Values of the parameters associated with the nucleon-nucleon scattering amplitude and with the projectile and target densities for the different reactions.

	σ_{NN} (fm^2)	α_{NN}	$\rho_0^P(0)$ (fm^{-3})	a_P (fm)	$\rho_0^T(0)$ (fm^{-3})	a_T (fm)	Ref.
^{12}C + ^{12}C, E_{lab}=360 MeV	19.6	0.87	0.0248	1.935	0.0248	1.935	13
^{12}C + ^{12}C, E_{lab}=1016 MeV	6.1	1.0	0.0248	1.935	0.0248	1.935	13
^{40}Ar + ^{208}Pb, E_{lab}=1760 MeV	12.5	0.93	0.01645	2.52	0.01245	3.45	14

The integral in (14) can, in general, only be expressed in terms of transcendent functions in the form

$$\mu_{LM}(b)=S_{LM}\frac{\Gamma[(M+L+2)/2]}{\Gamma(M+1)}\frac{2^{L+1}b^M}{[(a_T^2+a_P^2)^{L+M+2}]}\mathbf{M}\left[\frac{M+L+2}{2},M+1,-\frac{b^2}{a_P^2+a_T^2}\right], \tag{32}$$

in terms of the gamma function $\Gamma(z)$ and of the Kummer's confluent hypergeometric function $\mathbf{M}(a,b,z)$. The constant S_{LM} is defined as

$$S_{LM}=-2f_{NN}\frac{B_{LM}}{ik}\frac{\beta_L\rho_0^T(0)}{\sqrt{2L+1}}\rho_0^P(0)a_Ta_P^3\pi^3\left[\frac{a_T^2}{2}\right]^L. \tag{33}$$

In the case of multipolarity $L=2$, however, this formula reduces to the simple analytic expression

$$\mu_{L=2,M=\pm2}(b)=-4f_{NN}\frac{B_{LM}}{ik}\frac{a_T^5a_P^3}{(a_T^2+a_P^2)^3}\pi^3\rho_0^P(0)\frac{\rho_0^T(0)\beta_L}{\sqrt{2L+1}}b^2e^{-b^2/(a_T^2+a_P^2)}, \tag{34}$$

$$\mu_{L=2,M=0}(b)=-4f_{NN}\frac{B_{LM}}{ik}\frac{a_T^5a_P^3}{(a_T^2+a_P^2)^2}\pi^3\rho_0^P(0)\frac{\rho_0^T(0)\beta_L}{\sqrt{2L+1}}\left[1-\frac{b^2}{a_T^2+a_P^2}\right]e^{-b^2/(a_T^2+a_P^2)}. \tag{35}$$

As an application of the model we have considered the inelastic scattering of ^{12}C + ^{12}C (2^+; 4.4 MeV) at 360 and 1016 MeV. All the parameters for the nucleon-nucleon scattering and the ^{12}C densities [σ_{NN}, α_{NN}, $\rho_0(0)$,a] are taken as in Ref. 13 and are given in Table I. We remind that these parameters give a good description of the corresponding elastic scattering heavy-ion data.[13] The calculated inelastic cross sections are compared in Figs. 1 and 3 with the results of a DWBA calculation (solid line), whose optical parameters are given in Table II and also give a good account of the elastic data. Both prescriptions for the nucleon-projectile amplitude were used: the dashed line corresponds to the microscopic result given by formula (24), while the dotted line refers to the semimicroscopic formula (25). For a better internal comparison between the different approaches, we have used for each energy in all cases the same value of the dynamic deformation parameter β_L, chosen by normalizing to the data the first maximum of the DWBA angular distribution. For the comparison with the experimental data, displayed in Figs. 2 and 4, we have instead felt free to normalize separately the different curves, by using slightly different values of β_L (0.70 and 0.50 in the case of the Glauber model at the two energies and 0.93 and 0.715 in the corresponding DWBA calculation). Coulomb excitation was not taken into account in all cases, and this may be partly responsible for the value of β_L not exactly equal to the one obtained in the collective model from the experimental $B(E2)$ value.

In all cases, the angular distributions are in good agreement with both the experimental data and the DWBA calculations. This agreement is particularly remarkable

TABLE II. Values of the parameters defining the optical potential

$$U(r)=-\frac{V}{1+e^{\frac{r-r_V(A_T^{1/3}+A_P^{1/3})}{a_V}}}-\frac{iW}{1+e^{\frac{r-r_W(A_T^{1/3}+A_P^{1/3})}{a_W}}}$$

used in the DWBA calculations for the different reactions.

	V	r_V	a_V	W	r_W	a_W	Ref.
^{12}C + ^{12}C, E_{lab}=360 MeV	120.0	0.79	0.70	47.5	0.92	0.72	3
^{12}C + ^{12}C, E_{lab}=1016 MeV	120.0	0.71	0.84	34.02	0.96	0.69	3
^{40}Ar + ^{208}Pb, E_{lab}=1760 MeV	73.36	1.179	0.63	65.1	1.179	0.63	2

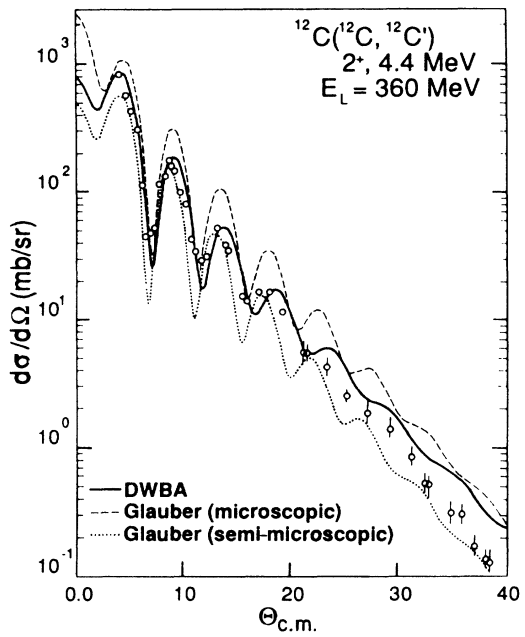

FIG. 1. Angular distribution for the inelastic excitation of the 2^+ state at 4.4 MeV in the $^{12}C + ^{12}C$ reaction at 360 MeV. Experimental data are taken from Ref. 3. The solid line is the prediction of the DWBA calculation, performed with the optical parameters given in Table II. The dashed and the dotted curves are the results of the Glauber model, obtained according to Eqs. (24) and (25), respectively. The parameters for the nucleon-nucleon scattering amplitude and for the nuclear densities are given in Table I. The collective model has been used to describe the excited state, with a value $\beta_L = 0.93$ in all the calculations. Only nuclear excitation has been taken into account.

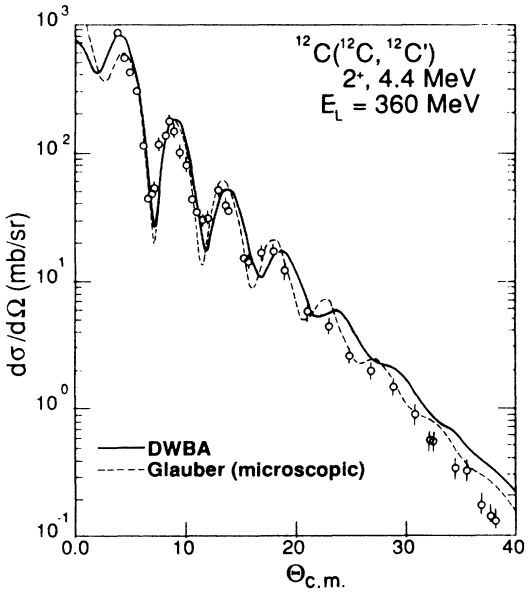

FIG. 2. Angular distribution for the inelastic excitation of the 2^+ state at 4.4 MeV in the $^{12}C + ^{12}C$ reaction at 360 MeV. Experimental data are taken from Ref. 3. The solid line is the prediction of the DWBA calculation, while the dashed line is the result of the Glauber model, obtained according to Eq. (24). The two curves have been separately normalized to the first peak, by using the values $\beta_L = 0.93$ and 0.70, respectively. For other details cf. caption to Fig. 1.

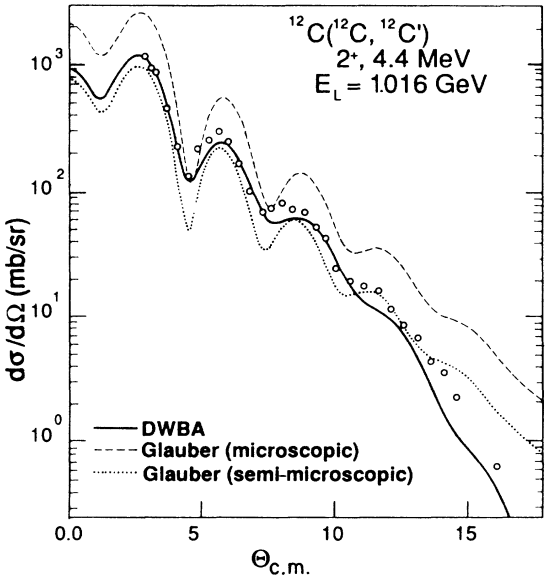

FIG. 3. Angular distribution for the inelastic excitation of the 2^+ state at 4.4 MeV in the $^{12}C + ^{12}C$ reaction at 1016 MeV. Experimental data are taken from Ref. 3. The solid line is the prediction of the DWBA calculation, performed with the optical parameters given in Table II. The dashed and the dotted curves are the results of the Glauber model, obtained according to Eqs. (24) and (25), respectively. The parameters for the nucleon-nucleon scattering amplitude and for the nuclear densities are given in Table I. The collective model has been used to describe the excited state, with a value $\beta_L = 0.715$ in all the calculations. Only nuclear excitation has been taken into account.

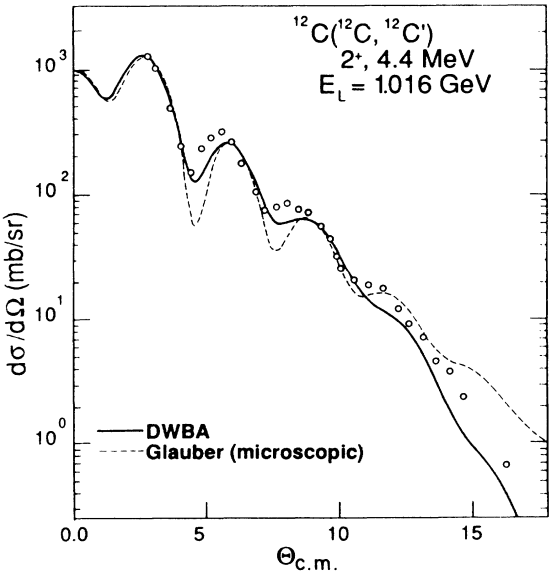

FIG. 4. Angular distribution for the inelastic excitation of the 2^+ state at 4.4 MeV in the $^{12}C + ^{12}C$ reaction at 1016 MeV. Experimental data are taken from Ref. 3. The solid line is the prediction of the DWBA calculation, while the dashed line is the result of the Glauber model, obtained according to Eq. (24). The two curves have been separately normalized to the first peak, by using the values $\beta_L = 0.715$ and 0.50, respectively. For other details cf. caption to Fig. 3.

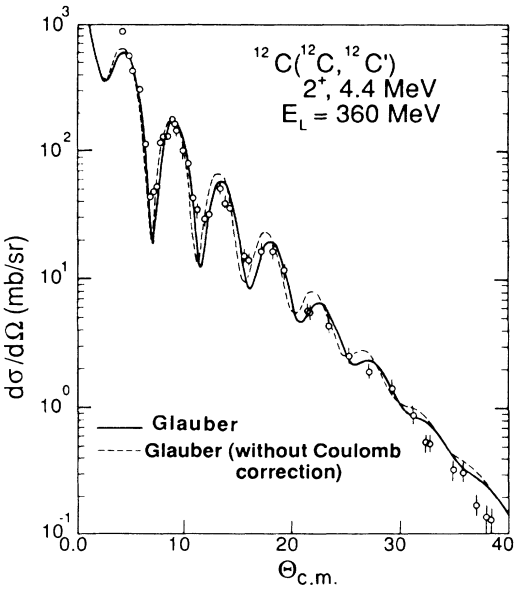

FIG. 5. Comparison of angular distributions obtained in the Glauber model for the inelastic excitation of the 2^+ state at 4.4 MeV in the $^{12}C + ^{12}C$ reaction at 360 MeV. The two curves have been obtained with (solid line) and without (dashed line) the correction for the Coulomb deflection [Eq. (23)]. In both cases the value $\beta_L = 0.70$ has been used. For other details cf. caption to Fig. 1.

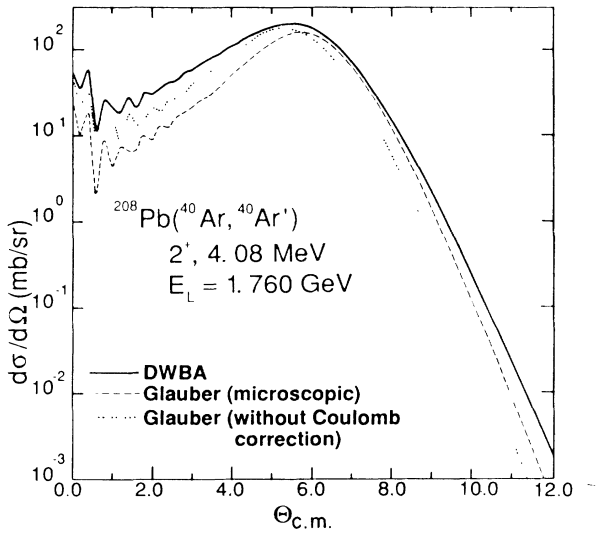

FIG. 6. Angular distribution for the inelastic excitation of the 2^+ state at 4.1 MeV in the $^{40}Ar + ^{208}Pb$ reaction at 1760 MeV. The solid line is the prediction of the DWBA calculation, while the dashed and dotted lines are the results of the full microscopic Glauber model, obtained with and without the correction for the Coulomb deflection, respectively. In all cases the value $\beta_L = 0.055$ has been used. For the parameters entering in the DWBA and Glauber calculations cf. Tables II and I, respectively.

in the forward-angle region where the Glauber approximation is expected to work better. The difference between the microscopic and semimicroscopic approaches is mainly in magnitude, so that the differential cross section of the second approach could be obtained from the first using a scaling factor which, in the spirit of Ref. 15, may be related to the effective number of nucleons participating in the nucleon-projectile collision. To better appreciate the quality of the fits, it is important to remind that the angular distributions calculated in the Glauber model are parameter-free predictions, only based on the experimental nucleon-nucleon data and the deformation parameter β_L.

The importance of the correction due to the distortion of the trajectory due to the Coulomb field is put into evidence by Fig. 5, where the predictions of the model with and without the correction are compared for the case of the lowest incident energy. No difference is, on the other hand, appreciable at the higher energy. The effect is, in fact, basically dependent on the value of the Sommerfeld parameter η, and therefore obviously expected to vanish in the high-energy limit.

We have up to now considered only inelastic processes in reactions involving relatively light ions, namely ^{12}C. As an example involving heavier systems, we consider now a model case associated with the excitation, through the nuclear field, of a 2^+ state in the $^{40}Ar + ^{208}Pb$ reaction at 1760 MeV. At variance with the previous cases characterized by diffractive angular distributions, this reaction is associated with a rather smooth bell-shaped angular distribution peaked around the grazing angle. It may also be worthwhile noticing that, due to the bombarding energy and the size of the colliding nuclei, the standard DWBA approach already involves a rather cumbersome calculation with a large number of partial waves ($l_g \approx 600$).

Angular distributions obtained within the DWBA (solid line) and the Glauber model (dashed line) are compared in Fig. 6. For the former we have used the optical parameters given in Table II and obtained by fitting the elastic angular distribution. For the latter we have used the parameters associated with the nucleon-nucleon scattering amplitude and with the projectile and target densities given in Table I, also previously successfully used to describe within the Glauber model the elastic scattering.[4] In both cases the value $\beta_L = 0.055$ has been used for the dynamical deformation parameter. The agreement between the DWBA and the Glauber calculation is rather fair, for both absolute magnitude and angular distribution. Note in particular the improvement originating from the shift in the grazing angle, due to the Coulomb correction.

[1]A. Lounis *et al.*, in *Proceedings of the International Conference on Nuclear Physics, Florence, 1983; Contributed Papers,* edited by B. Blasi and R. A. Ricci (Tipografia Composition, Bologna, 1983), p. 523; M. Buenerd *et al.*, *ibid.*, p. 524; N. Alamanos *et al.*, ibid., p. 525; M. Buenerd *et al.*, Phys. Rev. C **23**, 1299 (1982).
[2]N. Alamanos *et al.*, Phys. Lett. **137B**, 37 (1984).
[3]M. Buenerd *et al.*, Nucl. Phys. **A424**, 313 (1984).
[4]A. Vitturi and F. Zardi, Phys. Rev. C **36**, 1404 (1987).
[5]I. Ahmad, J. Phys. G **4**, 1695 (1978).
[6]T. S. Bauer *et al.*, Phys. Rev. C **19**, 1438 (1979).
[7]R. M. DeVries and J. C. Peng, Phys. Rev. C **22**, 1055 (1980); J. C. Peng, R. M. DeVries, and N. J. DiGiacomo, Phys. Lett. **98B**, 244 (1981); N. DiGiacomo, R. M. DeVries, and J. C. Peng, Phys. Rev. Lett. **45**, 527 (1980).
[8]W. Czyż and L. C. Maximon, Ann. Phys. **52**, 59 (1969); J. Formánek, Nucl. Phys. **B12**, 441 (1969).
[9]M. L. Goldberger and K. M. Watson, *Collision Theory* (Wiley, New York, 1964).
[10]J. M. Eisenberg, Ann. Phys. **71**, 542 (1972).
[11]A. Vitturi and F. Zardi, Lett. Nuovo Cimento **20**, 640 (1977).
[12]I. Ahmad, Nucl. Phys. **A247**, 418 (1975).
[13]J. Chanvin, A. Lebrun, A. Lounis, and M. Buenerd, Phys. Rev. C **28**, 1970 (1983).
[14]P. J. Karol, Phys. Rev. C **11**, 1203 (1975).
[15]G. F. Bertsch and O. Scholten, Phys. Rev. C **25**, 804 (1982).